The classical complement pathway is activated by allergen-specific pre-existing antibodies, and complement alternative pathway activation can be initiated directly by allergen polysaccharide structures. In addition, proteases directly activated by mite or mast cell tryptase or released by mucosal epithelial cells can generate complement split-product proteins during allergic reaction.[3] Bowser et al[8] first demonstrated that complement split products correlate with asthma severity and that changes in C3a and C5a levels reflect cutaneous allergic responses from dust mites after immunotherapy.

Downregulation of the effector T-cell response through development of a T-cell lineage with suppressive properties might be a novel role for complement in the contraction of an immune response.[4] The complement regulatory protein CD46 can induce the development of a distinct immunomodulatory T-cell population similar to adaptive IL-10–producing T_R1 cells.[5-7] Further understanding how CD46 activates IL-10–producing T_R1 cells during *D pteronyssinus* SIT and the dose of mite allergens might be important. The total dust mite SIT dosage has been reported to be associated with changes in C5a and C3a levels, and this might be due to activation of the complement activation by *D pteronyssinus* proteases, endotoxin, or both in multiple allergen extracts.[8]

CD3/CD46-activated T_R1-like cells permit dendritic cell activation through their simultaneous secretion of GM-CSF and soluble CD40, which could be desirable in mucosal tolerance.[9] In the airway the cytokine profile of complement-activated Treg cells might ensure unresponsiveness to allergen-mediated complement activation by suppressing an unwanted T-cell response through IL-10 while maintaining reactivity to invading pathogens.[6]

In summary, we have provided evidence that *D pteronyssinus* SIT can enhance the suppressive function of IL-10/IFN-γ in CD3/CD46-activated T_R1-like cells from asthmatic patients, and this might explain the dysfunctional ability of Treg cells to suppress mite-induced airway epithelial cell inflammation. On the basis of these results, it might be possible to design therapeutic strategies to manipulate the complement-activated Treg cells to achieve allergen tolerance and suppress airway inflammation in patients with allergic asthma.

Yi-Giien Tsai, MD, PhD[a,b]
Jui-Chung Lai, MD[c]
Kuender D. Yang, MD, PhD[d,e]
Chih-Hsing Hung, MD, PhD[f]
Ya-Ju Yeh, MS[a]
Ching-Yuang Lin, MD, PhD[g]

From [a]the Department of Pediatrics, Changhua Christian Hospital, School of Medicine, Kaohsiung Medical University, Taiwan; [b]the School of Medicine, Chung Shan Medical University, Taichung, Taiwan; [c]the Department of Otorhinolaryngology, Head and Neck Surgery, Changhua Christian Hospital, Changhua, Taiwan; [d]the Department of Medical Research and Development, Show Chwan Memorial Hospital, Chang Bing, Taiwan; [e]the Institute of Clinical Medicine, National Yang Ming University, Taipei, Taiwan; [f]the Department of Pediatrics, Kaohsiung Medical University Hospital, Kaohsiung Medical University, Kaohsiung, Taiwan; and [g]the Clinical Immunological Center, China Medical University Hospital, College of Medicine, China Medical University, Taichung, Taiwan. E-mail: cylin@mail.cmuh.org.tw.

Supported in part by grants from the National Science Council, Taiwan, ROC (NSC 101-2314-B-371-001 and NSC 102-2314-B-371-001) and grants from Changhua Christian Hospital (102-CCH-IRP-031 and 103-CCH-IRP-032).

Disclosure of potential conflict of interest: The authors declare that they have no relevant conflicts of interest.

REFERENCES

1. Akdis CA, Akdis M. Mechanisms of allergen-specific immunotherapy: multiple suppressor factors at work in immune tolerance to allergens. J Allergy Clin Immunol 2014;133:621-31.
2. Tsai YG, Chiou YL, Chien JW, Wu HP, Lin CY. Induction of IL-10+ CD4+CD25+ regulatory T cells with decreased NF-kappaB expression during immunotherapy. Pediatr Allergy Immunol 2010;21:e166-73.
3. Laumonnier Y, Schmudde I, Köhl J. The role of complement in the diagnosis and management of allergic rhinitis and allergic asthma. Curr Allergy Asthma Rep 2011;11:122-30.
4. Riley-Vargas RC, Gill DB, Kemper C, Liszewski MK, Atkinson JP. CD46: expanding beyond complement regulation. Trends Immunol 2004;25:496-503.
5. Astier AL, Meiffren G, Freeeman S, Hafler DA. Alterations in CD46-mediated Tr1 regulatory T cells in patients with multiple sclerosis. J Clin Invest 2006;116:3252-7.
6. Tsai YG, Niu DM, Yang KD, Hung CH, Yeh- YJ, Lee CY, et al. Functional defects of CD46-induced regulatory T cells to suppress airway inflammation in mite allergic asthma. Lab Invest 2012;92:1260-9.
7. Xu YQ, Gao YD, Yang J, Guo W. A defect of CD4+CD25+ regulatory T cells in inducing interleukin-10 production from CD4+ T cells under CD46 costimulation in asthma patients. J Asthma 2010;47:367-73.
8. Bowser C, Erstein DP, Silverberg JI, Nowakowski M, Joks R. Correlation of plasma complement split product levels with allergic respiratory disease activity and relation to allergen immunotherapy. Ann Allergy Asthma Immunol 2010;104:42-9.
9. Barchet W, Price JD, Cella M, Colonna M, MacMillan SK, Cobb JP, et al. Complement-induced regulatory T cells suppress T-cell responses but allow for dendritic-cell maturation. Blood 2006;107:1497-504.

Available online July 25, 2014.
http://dx.doi.org/10.1016/j.jaci.2014.06.005

Gain-of-function mutations in signal transducer and activator of transcription 1 (*STAT1*): Chronic mucocutaneous candidiasis accompanied by enamel defects and delayed dental shedding

To the Editor:

Heterozygous gain-of-function mutations in signal transducer and activator of transcription 1 *(STAT1)* have recently been identified as a cause of chronic mucocutaneous candidiasis (CMC). Uzel et al[1] described "*STAT1* gain-of-function mutations in patients with *FOXP3* wild-type immune dysregulation-polyendocrinopathy-enteropathy-X-linked syndrome." They briefly mentioned the presence of poor enamel in 1 patient and structural and functional gastrointestinal defects in another patient. Here we present a patient with CMC associated with dental anomalies, diaphragmatic hernia, and esophageal dysmotility in whom the phenotype led to a broad differential diagnosis ranging from severe combined immunodeficiency inspired by the neonatal onset of infections to humoral immune deficiency, immune dysregulation–polyendocrinopathy–enteropathy–X-linked syndrome, nuclear factor κB essential modulator *(NEMO)* deficiency, Shwachman-Diamond syndrome, autosomal dominant hyper-IgE syndrome, and, finally, CMC caused by gain-of-function mutation in *STAT1*. We stress the early onset of respiratory tract infections, as well as the dental and gastrointestinal defects, in this patient.

The patient was born at term small for gestational age (−2 SD) as the third son of unrelated parents. He presented with recurrent lower respiratory tract infections from birth, intractable diarrhea, failure to thrive, seborrheic dermatitis, and CMC. Small-bowel

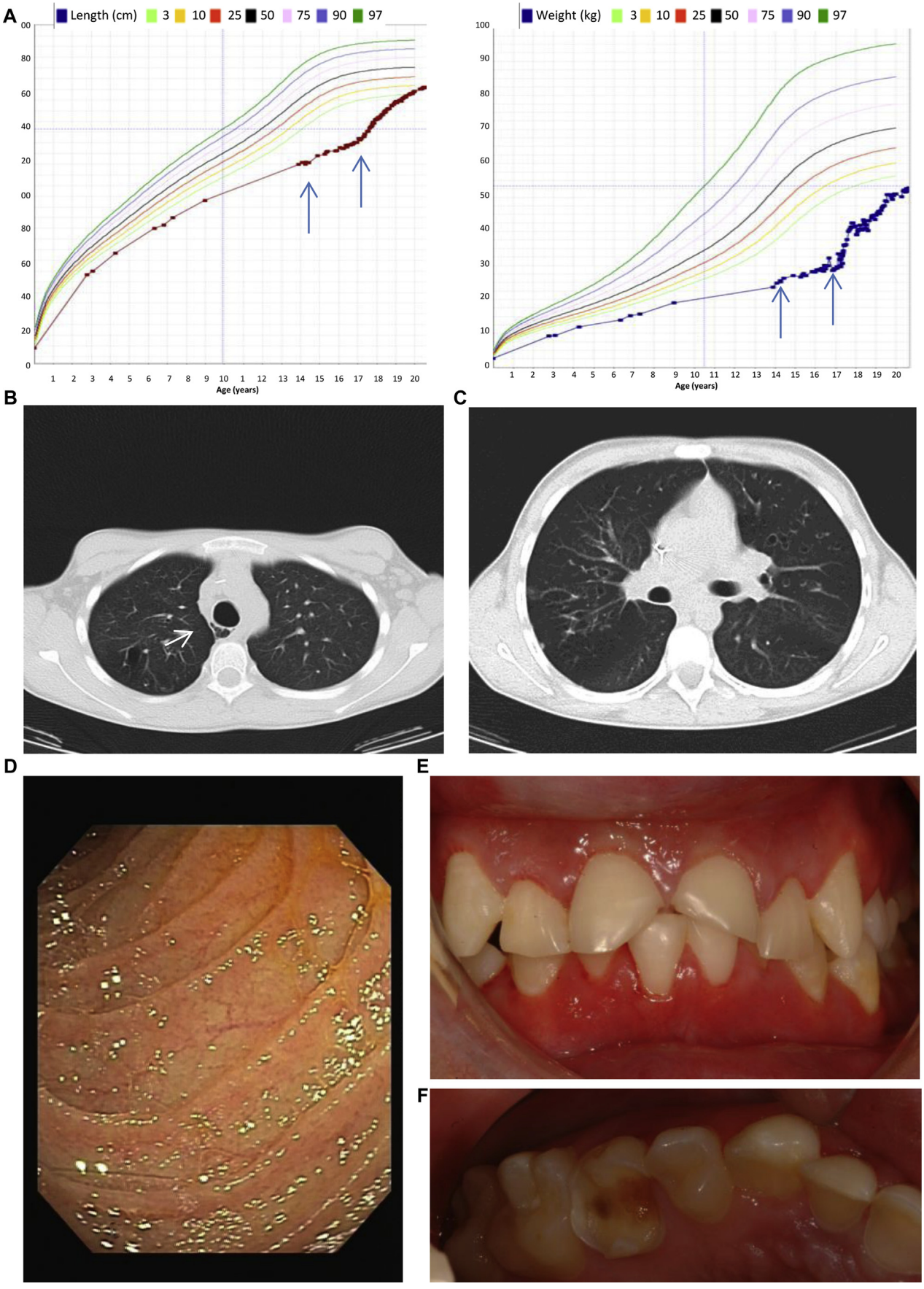
A
Length (cm) 3 10 25 50 75 90 97
Age (years)
Weight (kg) 3 10 25 50 75 90 97
Age (years)
B
C
D
E
F

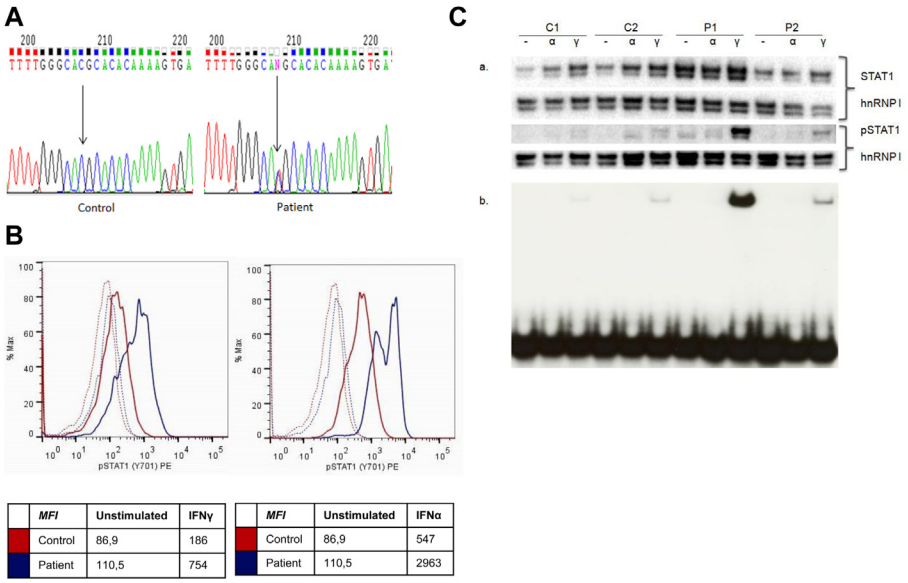

	MFI	Unstimulated	IFNγ
	Control	86,9	186
	Patient	110,5	754

	MFI	Unstimulated	IFNα
	Control	86,9	547
	Patient	110,5	2963

FIG 2. The mutant T385M *STAT1* allele is a gain-of-phosphorylation and gain-of-function mutation. **A,** Direct sequence analysis of exon 14 of *STAT1* (forward sequence) in a control subject and the patient with a c.1153C>T resulting in p.T385M. **B,** Intracellular staining of phosphorylated tyrosine 701 STAT1 *(STAT1p)* in lymphocytes after stimulation with IFN-γ (2000 IU/mL, *left panel*) or IFN-α (10^5 IU/mL, *right panel*) for 15 minutes. STAT1 and STATp are shown in a control subject (red) and in the T385M patient *(blue)*. Unstimulated conditions are represented as *dashed lines*. Results shown are representative of 2 independent experiments. *MFI*, Mean fluorescence intensity. **C,** Evaluation of STAT1, STAT1 phosphorylation, and STAT1p GAS DNA-binding capacity. Fibroblasts derived from wild-type (WT)/WT control subjects (C1 and C2), p.T385M/WT (patient P1), and p.K388E/WT (patient P2) were stimulated with 100 U/mL IFN-α *(α)* or 100 U/mL IFN-γ *(U)* or left unstimulated *(−)* for 60 minutes. *a*, Western blotting was carried out for detection of STAT1 and STAT1p levels in nuclear extracts (5 μg per sample). Heterogeneous nuclear ribonucleoprotein I (hnRNP I) was used as a loading control reference. *b*, STAT1 GAS DNA-binding capacity was evaluated by using EMSA. One microgram of nuclear extract was preincubated with 20,000 cpm of GAS probe at room temperature before nondenaturing PAGE separating free from STAT-bound probe.

biopsy showed villous atrophy interpreted as celiac-like disease, yet diarrhea was unresponsive to a gluten-free diet. Primary dentition showed enamel defects. Recurrent lower respiratory tract infections with *Haemophilus influenzae and Streptococcus pneumoniae* led to the development of bronchiectasis. Partial IgG_2 deficiency (0.34 g/L; normal range, 0.72-3.4 g/L) was found at 3 years of age. Anti-tetanus antibody levels were protective (1.2 mg/L; protective level, >1 mg/L), suggesting an intact anti-protein antibody response. Intravenous immunoglobulin (IVIG) substitution was initiated. Diaphragmatic hernia, gastroesophageal reflux disease, and disturbed esophageal motility were demonstrated and led to a Nissen fundoplication.

At 13 years of age, the patient presented at the immunology clinic with severe growth retardation (Fig 1, *A*), pubertal delay, bronchiectasis, atonic esophagus with multiple diverticula (Fig 1, *B* and *C*), atrophic duodenal mucosa (Fig 1, *D*) corresponding to villous blunting or atrophy, joint hyperlaxity, osteopenia with recurrent fractures, delayed dental development with retention of primary teeth necessitating dental extractions (Fig 1, *E* and *F*), severe erosive tooth wear suggestive of enamel hypoplasia (Fig 1, *E* and *F*), seborrheic dermatitis, aphthous stomatitis, and CMC (see Table E1 in this article's Online Repository at www.jacionline.org). The autoimmune regulator *(AIRE)* and caspase recruitment domain family, member 9 *(CARD9)*, genes were sequenced, but no mutations were found. After withdrawal of IVIG, antibody response to unconjugated pneumococcal vaccine was tested and showed protective titers for 9 of 14 serotypes tested (see Table E2 in this article's Online Repository at www.jacionline.org).[2] Increased IgG levels (21 g/L; normal range, 5.76-12.65 g/L) and persistent partial IgG_2 deficiency were noted (0.80 g/L; normal range, 1.06-6.10 g/L). An extended autoantibody screening panel was performed, including thyroid-related, adrenal gland–related, and anti–IFN-α and anti–IFN-ω antibodies. Only anti–salivary gland antibodies were demonstrated (for the entire panel, see the Methods section in this article's Online Repository at www.jacionline.org). Immunophenotyping showed a low percentage of switched memory B cells (1.3%; normal range, 5% to 10%; see Table E3 in this article's Online Repository at www.jacionline.org). Because withdrawal of IVIG was associated with an increased incidence of pneumonia, treatment was optimized by restarting IVIG and initiating azithromycin (both

FIG 1. Clinical characteristics. **A,** Growth charts showing severe growth retardation that only picks up after growth hormone therapy and puberty induction with tube feeding overnight. *Arrows* indicate onset of tube feeding and growth hormone therapy, respectively. **B,** Computed tomography showing an atonic esophagus *(arrow)* with air containing paraesophageal diverticula. **C,** Computed tomography of the chest showing multiple saccular bronchiectases and bronchial wall thickening. **D,** Atrophy in the duodenum, as seen on endoscopy. **E** and **F,** Severe erosive tooth wear, caries, and retained primary teeth.

for antibacterial prophylaxis and its anti-inflammatory actions) and fluconazole prophylaxis, as well as overnight tube feeding. Growth hormone therapy and puberty induction led to a correction of the growth deficit (Fig 1, *A*). Finally, at the age of 18 years, hypothyroidism was diagnosed almost simultaneously with the initial reports on *STAT1* coiled-coil domain gain-of-function mutations.[3,4] A mutation in the DNA-binding domain of *STAT1* was detected (c.1154C>T, p.T385M; Fig 2, *A*; for information on the analysis, see the Results section in this article's Online Repository at www.jacionline.org). The mutation was not found in the parents or the 2 male siblings of the index patient. As described previously, T385M is a gain-of-function mutation.[1,5-7] Likewise, we showed increased STAT1 phosphorylation in response to IFN-α and IFN-γ in the patient compared with control values (Fig 2, *B*). Also, the electrophoretic mobility shift assay (EMSA) showed increased gamma-activated sequence (GAS) binding activity on stimulation with IFN-γ (Fig 2, *C*).

The mechanism that leads to gain of function in the T385M mutation is not entirely clear. Takezaki et al[5] suggested an impaired dephosphorylation of STAT1. However, it is also possible that there is impaired dissociation from the DNA or a problem with the reciprocal association of the DNA-binding domain with the coiled-coil domain. After diagnosis, extended immunophenotyping of PBMCs was performed and showed absence of T_H17 cells, as described by Liu et al.[4]

The dental anomalies in the patient were impressive. Both primary and permanent teeth showed rapid loss of tooth substance, with severe caries and erosive tooth wear reminiscent of the dental anomalies encountered in patients with Shwachman-Diamond syndrome or Ora1/Stromal interaction molecule 1 deficiency. Moreover, deciduous teeth had to be extracted because of delayed shedding. The latter feature resembles autosomal dominant hyper-IgE syndrome.

Several hypotheses to explain the dental anomalies were put forward. First, antibiotic and antimycotic therapy and acidic hypercaloric nutrition were blamed. Second, malabsorption of calcium and vitamin D was investigated. Third, in the context of recurrent aphthous stomatitis, a sicca syndrome was suspected. Although salivary flow was low, treatment with oral saliva analogues did not improve the dental condition. There were no biochemical or clinical signs of hypothyroidism until age 18 years in our patient, excluding this as a cause for the delayed shedding of deciduous teeth. Although a role for *STAT1* signaling has been demonstrated in amelogenesis and dentinogenesis in rats, further research is needed to investigate the potential causal relationship between *STAT1* gain-of-function mutation and abnormal dental development.[8,9]

Aside from the persistent villous blunting, diaphragmatic hernia and esophageal dysmotility are remarkable gastrointestinal features. On computed tomographic (CT) scanning, as well as endoscopy, the esophagus appeared wide open and atonic, with multiple diverticula present. Thus defects in the development of the upper gastrointestinal tract seem to be a noteworthy feature of this syndrome, as hypothesized by Uzel et al.[1] Whether the gastrointestinal manifestations are all secondary to CMC or a primary manifestation of disturbed *STAT1* signaling is yet to be determined.[1,6]

In conclusion, we report extensive dental anomalies, as well as diaphragmatic hernia and esophageal dysmotility, in a patient with early onset of lower respiratory tract infections in the context of a gain-of-function mutation in the DNA-binding domain of *STAT1*. These features add to the complexity of the phenotype observed in patients with a gain-of-function mutation in *STAT1*.

We thank the patient and his family for their confidence. We also thank the entire paramedical and medical staff of UZ Leuven, as well as Dr De Koster, for their dedicated care. Finally, we thank Mrs R. Bollen and H. De Bruyn for excellent technical assistance.

Glynis Frans, MPharm[a]*
Leen Moens, PhD[a]*
Heidi Schaballie, MD[a,g]
Lien Van Eyck, MD, MSc[b,g]
Heleen Borgers, PhD[a]
Margareta Wuyts, BSc[a]
Doreen Dillaerts, MSc[a]
Edith Vermeulen, MPharm[c]
James Dooley, PhD[b]
Bodo Grimbacher, MD, PhD[d]
Andrew Cant, MD, PhD[e]
Dominique Declerck, PhD[f]
Marleen Peumans, PhD[f]
Marleen Renard, MD[g]
Kris De Boeck, MD, PhD[g]
Ilse Hoffman, MD, PhD[g]
Inge François, MD, PhD[g]
Adrian Liston, PhD[b]
Frank Claessens, MD, PhD[h]
Xavier Bossuyt, MD, PhD[a]
Isabelle Meyts, MD, PhD[a,g]

From [a]the Department of Microbiology and Immunology, Experimental Laboratory Immunology, Katholieke Universiteit Leuven, Leuven, Belgium; [b]the Laboratory Genetics of Autoimmunity, Vlaams Instituut Biotechnologie, Leuven, Belgium; [c]the Department of Microbiology and Immunology, Laboratory for Clinical Bacteriology and Mycology, Katholieke Universiteit Leuven, Leuven, Belgium; and [d]the Centre for Chronic Immunodeficiency, University Hospital Freiburg, Freiburg, Germany; [e]the Primary Immunodeficiency Group, Institute of Cellular Medicine, Newcastle University and Pediatric Immunology Service, Great North Children's Hospital, Newcastle upon Tyne, United Kingdom; [f]the Department of Conservative Dentistry, School for Dentistry, Katholieke Universiteit Leuven, University Hospitals Leuven, Leuven, Belgium; [g]the Department of Pediatrics, University Hospitals Leuven, Leuven, Belgium; and [h]the Department of Cellular and Molecular Medicine, Laboratory of Molecular Endocrinology, Katholieke Universiteit Leuven, Leuven, Belgium. E-mail: Isabelle.Meyts@uzleuven.be.

*These authors contributed equally to this work.

Supported by a research grant from the Fonds Wetenschappelijk Onderzoek - Vlaanderen and by a research grant from the Research Council of the Catholic University of Leuven. X.B. is a senior clinical investigator of the Fonds Wetenschappelijk Onderzoek - Vlaanderen. I.M. is funded by a K.O.F. grant of the Katholieke Universiteit Leuven and by a grant of the Jeffrey Modell Foundation. L.M., H. S., and L.V.E. are funded by a research grant of the Fonds Wetenschappelijk Onderzoek - Vlaanderen. X.B., I.M., A.L., and G.F. are funded by a G.O.A. grant of the Katholieke Universiteit Leuven. A.L. is funded by a European Research Council grant (IMMUNO).

Disclosure of potential conflict of interest: G. Frans has received research support from the Catholic University of Leuven. L. Moens, H. Schaballie, and E. Vermeulen have received research support from Fonds Wetenschappelijk Onderzoek - Vlaanderen. L. Van Eyck has received research support from Fonds Wetenschappelijk Onderzoek - Vlaanderen and is employed by University Hospital Leuven. J. Dooley and A. Listons have received research support from the European Research Council. B. Grimbacher has received research support from the German Federal Ministry of Education and Research, the European Union, and Helmholtz; is employed by University College London and University Medical Center Freiburg; and has received payment for lectures from CSL, Baxter, and Biotest. M. Renard is employed by University Hospital Leuven. K. De Boeck serves on boards for Vertex, Aptalis, and Pharmaxix and has consultant arrangements with Ablynx, Galapagos, Gilead, and PTC. I. Meyts has received financial support from the Jeffrey Modell Foundation. The rest of the authors declare that they have no relevant conflicts of interest.

REFERENCES

1. Uzel G, Sampaio EP, Lawrence MG, Hsu AP, Hackett M, Dorsey MJ, et al. Dominant gain-of-function *STAT1* mutations in *FOXP3* wild-type immune dysregulation-polyendocrinopathy-enteropathy-X-linked-like syndrome. J Allergy Clin Immunol 2013;131:1611-23.
2. Borgers H, Moens L, Picard C, Jeurissen A, Raes M, Sauer K, et al. Laboratory diagnosis of specific antibody deficiency to pneumococcal capsular polysaccharide antigens by multiplexed bead assay. Clin Immunol 2010;134:198-205.
3. van de Veerdonck FL, Plantinga TS, Hoischen A, Smeekens SP, Joosten LAB, Gilissen C, et al. *STAT1* mutations in autosomal dominant chronic mucocutaneous candidiasis. N Engl J Med 2011;365:54-6.
4. Liu L, Okada S, Kong X, Kreins A, Cypowyj S, Abhynkar A, et al. Gain-of-function human *STAT1* mutations impair IL-17 immunity and underlie chronic mucocutaneous candidiasis. J Exp Med 2011;208:1635-48.
5. Takezaki S, Yamada M, Kato M, Park M, Maruyama K, Yamazaki Y, et al. Chronic mucocutaneous candidiasis caused by a gain of function mutation in the STAT1 DNA binding domain. J Immunol 2012;189:1521-6.
6. Soltesz B, Toth B, Shabahova N, Bondarenko A, Okada S, Cypowyj S, et al. New and recurrent gain-of-function STAT1 mutations in patients with chronic mucocutaneous candidiasis from Eastern and Central Europe. J Med Genet 2013;50:567-78.
7. Sampaio EP, Hsu AP, Pechacek J, Bax HI, Dias DL, Paulson ML, et al. Signal transducer and activator of transcription 1 (STAT1) gain-of-function mutations and disseminated coccidioidomycosis and histoplasmosis. J Allergy Clin Immunol 2013;131:1624-34.
8. Otsuji W, Tanase S, Yoshida S, Bawden JW. The immunohistochemical localization of the interferon-gamma and granulocyte colony stimulating factor receptors during early amelogenesis in rat molars. Arch Oral Biol 1999;44:173-81.
9. Tanase S, Bawden JW. The immunohistochemical localization of signal-transduction pathway components Jak1, Jak2, Jak3, Tyk2 and *STAT1* during early enamel and dentine formation in rat molars. Arch Oral Biol 1996;41:925-40.

Available online July 18, 2014.
http://dx.doi.org/10.1016/j.jaci.2014.05.044

Transmission of allergen-specific IgG and IgE from maternal blood into breast milk visualized with microarray technology

To the Editor:

Data from experimental animal models have previously shown that allergen-specific IgG antibodies are transmitted from the mother to the offspring via breast milk[1,2] and have provided evidence that the transmitted allergen-specific IgG antibodies protect specifically against allergic sensitization.[2] In some studies, it has been demonstrated for humans that breast-feeding has a prophylactic effect against atopic disease but there are also reports arguing against this and the underlying mechanisms are not known.[3] There is evidence that IgG antibodies against bacterial antigens (ie, pneumococcal antigens) are transferred from the blood of mothers into their breast milk.[4] Furthermore, it was possible to detect IgA and IgG against different food antigens in human serum, saliva, colostrums, and milk samples.[5] Another study found that total IgE levels in breast milk and blood were associated but allergen-specific IgE was not analyzed.[6]

With the FP7-funded European Union research program Mechanisms of the Development of ALLergy (MeDALL; http://medall-fp7.eu/), we have recently developed a microarray containing a large number of purified natural and recombinant respiratory, food, and insect allergens that allows highly sensitive measurement of allergen-specific IgE and IgG levels with minute amounts of blood.[7] A major advantage of the microarray technology is that it allows one to measure antibody reactivities toward a large panel of different allergens. Here, we investigated whether the MeDALL chip is suitable for (1) the measurement of allergen-specific IgG and IgE levels in human breast milk samples, (2) whether there is a transmission of allergen-specific antibodies from blood into breast milk, and (3) whether the reactivity profile of allergens recognized by antibodies in blood and milk is similar. For this purpose, we analyzed plasma and breast milk samples from sensitized (n = 23) and nonallergic mothers (n = 6) from the ALADDIN birth cohort.[8] None of the mothers was on allergen-specific immunotherapy. Maternal blood samples were collected in the period around delivery (−1 to +2 months), and the breast milk samples were obtained 2 months after delivery. The study was approved by the local Research Ethical Committee, and written informed consent was obtained from all families.

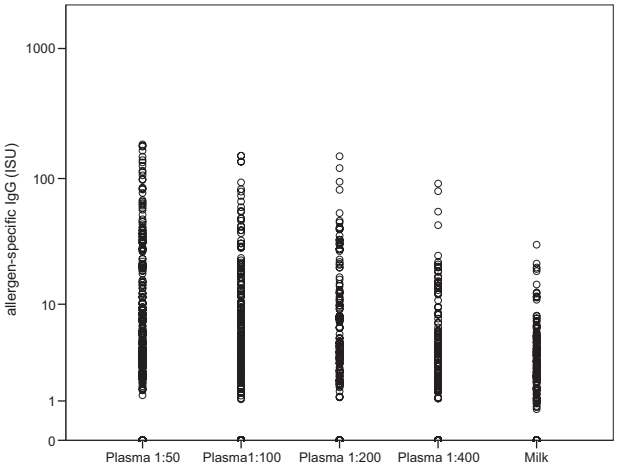

FIG 1. Comparison of allergen-specific IgG levels (ISAC standardized unit [ISU]) measured in different plasma dilutions of 4 mothers with allergen-specific IgG levels in their breast milk samples.

The breast milk samples were centrifuged for 10 minutes at 2500*g* before use to remove the lipids. For comparison of IgG titers in plasma and breast milk, the plasma samples were diluted 1:50, 1:100, 1:200, and 1:400 before analysis. Microarrays were incubated with 30 μL of the plasma dilutions or undiluted breast milk samples and allergen-specific IgG and IgE antibodies were detected with fluorophore-conjugated anti-IgG and anti-IgE antibodies, respectively.[7] The fluorescence intensities were measured with a biochip scanner. Results were expressed in ISAC standardized units (Thermofisher, Uppsala, Sweden). Correlation coefficients were calculated with SPSS.

Detailed analysis of allergen-specific IgG and IgE levels in plasma and breast milk samples indicated that allergen-specific IgG antibodies are transmitted from the blood into breast milk in a highly specific manner and that breast milk IgG mirrored the profile of IgG reactivity in the blood (see Fig E1 in this article's Online Repository at www.jacionline.org). A comparison of allergen-specific IgG levels measured in 4 plasma dilutions with that of undiluted breast milk samples (Fig 1) indicated that allergen-specific IgG levels in breast milk were approximately 200- to 400-fold lower than in plasma. Allergen-specific IgG reactivities in plasma and breast milk were significantly correlated; for the 1:200 dilution, Spearman correlation coefficient was 0.608 ($P < .001$) and for the 1:400 dilution, Spearman correlation coefficient was 0.604 ($P < .001$) (Fig 2). Detailed results are displayed

METHODS

Measurement of salivary flow rate

Salivary flow rate was measured through standardized collection of nonstimulated (resting) and stimulated (paraffin-chewing) saliva over a time span of 5 minutes.

Autoantibody analysis

The autoantibody panel analyzed consisted of anti–nuclear antigen, anti–neutrophil cytoplasmic, anti-thyroglobulin, anti–thyroid peroxidase, anti–thyrotropin receptor, anti–parietal cell, anti–intrinsic factor, anti–smooth muscle, anti-mitochondrial, anti-pancreatic, anti-insulin, anti-GAD65kDA, anti–liver kidney microsome, anti–proteinase 3, anti-myeloperoxidase, and anti–IFN-α and anti–IFN-ω antibodies. The latter analysis was performed by Anette S. Boe Wolff and Husebye Eystein, Bergen, Norway, because of the diagnostic value in patients with autoimmune polyendocrine syndrome type 1.[E1]

Genetic analysis

Genomic DNA was extracted from EDTA blood by using the QIAamp DNA Blood Mini Kit (Qiagen, Hilden, Germany). The UM13F/R-tagged primers (Life Technologies, Ghent, Belgium) used for genotyping *STAT1* hotspots (gene ID 6772, ENSG00000115415) were designed with Oligo7 software (OLIGO Primer Analysis Software Version 7, assembled in 2009 by Wojciech Rychlik, Molecular Biology Insights, Cascade, Colo; http://www.oligo.net/) and were as follows, respectively: AGTACAATAAAG TAAACATTCTGC (F1) and CTAAATCTGATTCTCCCACTT (R1); AGT CACACCCTGAAGAAAACGATG (F2) and CTGCAAAATTTTTCTTCC CAA (R2); AGTCTAAAGTCTTTGGAAGTTGCT (F3) and CTGGCCT GGGTTATCAAGGAA (R3); AGTTCTTCTTTATATATTTACTGG (F4) and GGTGGCTATAATTTTTCCTCT (R4); AGTTGAGAATGAAATGA TATTTGC (F5) and GTGTTTATGTGGTTAGCCAGT (R5); AGTCTTCTG GACTGTTTCTCATAG (F6) and ATCATCTGAATTAACGGTAAA (R6); AGTCCTCAACCTTAATGGAAATGC (F7) and CTCAAAAGCACCCTA TATAAC (R7); AGTAAACGTTAATAGGGAATTGGC (F8) and CCTAGG GAGGCAAACTTCCAC (R8); and AGTCTCTTATAATTTTGTTAAAGC (F9) and CCTACCAGGTGCCGAAATTCA (R9).

PCR samples were prepared by using AccuPrime SuperMix II (Life Technologies, Belgium) and run on a Veriti Thermal Cycler (Applied Biosystems, Foster City, Calif). Purified PCR products (PCR purification kit, Qiagen) were sequenced by BaseClear (Leiden, The Netherlands) and analyzed with Chromas 2.33 Software.

Analysis of phosphorylated STAT1 by using flow cytometry

Peripheral blood was left unstimulated or stimulated with IFN-γ (2000 IU/mL) or IFN-α (10*5 IU/mL) for 15 minutes. Cells were lysed (Lyse/Fix Buffer; BD Phosflow; BD Biosciences, San Jose, Calif) for 10 minutes at 37°C and washed with 1 mL of Stain Buffer (BD PharMingen, San Jose, Calif). Thereafter, the cells were permeabilized (Perm Buffer III [BD Phosflow]) for 30 minutes on ice. Cells were washed, resuspended in 100 μL of stain buffer, and stained with phycoerythrin-labeled antibody specific for phosphorylated STAT1 (pY701; BD Biosciences). Phosphorylated STAT1 was evaluated in the lymphocyte gate. Analysis was performed on a FACSCanto II instrument (BD Biosciences).

Western blot analysis

Nuclear extracts of patient- or control subject–derived fibroblast (obtained from skin biopsy) cultures (unstimulated or stimulated with IFN-α [100 U/mL] or IFN-γ [100 U/mL] for 1 hour) were prepared, as described previously.[E2] Nuclear protein lysates (5 μg per sample) were subjected to SDS-PAGE separation on 4-12% Bis-Tris Plus gels (Life Technologies, Carlsbad, Calif), and proteins were transferred to a polyvinylidene difluoride membrane (GE Healthcare, Buckinghamshire, United Kingdom) and immunoblotted with primary antibodies (STAT1 p84/p91 [M-22, sc-592; Santa Cruz Biotechnology, Dallas, Tex], phospho-STAT1 [Tyr701, sc-7988, Santa Cruz Biotechnology], and loading control heterogeneous nuclear ribonucleoprotein I [3H7, sc-73391, Santa Cruz Biotechnology]) and detected with horseradish peroxidase–conjugated secondary antibody (sc-2317 and sc-2005, Santa Cruz Biotechnology). All Western blot images were captured and quantified with a ChemiDoc MP imager and Image Lab software (Bio-Rad Laboratories, Hercules, Calif) after adding Pierce ECL Western blotting substrate (Thermo Scientific, Waltham, Mass). Relative phosphorylated STAT1 expression is normalized to the respective value for heterogeneous nuclear ribonucleoprotein I expression, and the results are described as fold increases relative to the baseline level in the unstimulated condition of the sample.

EMSA

EMSA was performed, as described previously.[E2] Probe (20,000 cpm) was added to 1 μg of nuclear extract in 50 ng/μL dI-dC, 1 mmol/L dithiothreitol, and 0.05% Triton. EMSA results with nonstimulated extracts or extracts stimulated with IFN-α or IFN-γ were compared. The GAS probe (5′-TCGAA CATTTCCCGTAAATCATG-3′, Chapgier et al[E3]) was labeled by a fill-in reaction with the Klenow fragment. EMSA results with nonstimulated extracts (dimethyl sulfoxide vehicle treated) or extracts stimulated with IFN-α (100 U/mL) or IFN-γ (100 U/mL) were compared in 2 control subjects (C1 and C2), the T385M patient (P1), and a patient with CMC with a K388E mutation in the DNA-binding domain (P2). Intensities of GAS-binding activity were determined by using ImageJ software.[E4]

Stimulation of PBMCs and measurement of cytokines

PBMCs were prepared from heparinized peripheral blood by means of centrifugation through Ficoll (Lymphoprep, Axis-shield, Oslo, Norway). PBMCs were seeded at 2×10^6 cells/mL in a 96-well culture plate and stimulated with heat-inactivated *Candida albicans* (2.64×10^3 colony-forming units [CFU]/mL), *Staphylococcus aureus* (10^8 CFU/mL; InvivoGen, San Diego, Calif), or PHA (0.18 mg/mL). IFN-γ levels were measured in the supernatant after 48 hours of incubation at 37°C (5% CO_2) and IL-17A levels were measured after 120 hours of incubation at 37°C (5% CO_2) by means of ELISA (commercial kits by BD Biosciences and BioLegend [San Diego, Calif], respectively). For the production of heat-inactivated *C albicans*, reference strain ATCC 90028 was used. This strain was cultured on Sabouraud agar slants at 37°C. Yeast colonies were resuspended in RPMI agar and checked microscopically for the absence of hyphae. This yeast stock suspension was adjusted to a concentration of 0.4×10^7 CFU/mL. *C albicans* was subsequently heat killed by exposure to a 60°C water bath for 1.5 hours. The sterility of this suspension was checked by subculturing 50 μL of the yeast suspension on blood agar at 37°C.

Immune response to Pneumovax

Antibodies to pneumococcal polysaccharides were measured by using a mulitplex bead assay.[E5]

Extended peripheral blood immunophenotying panel

PBMC immunophenotyping was performed, as described previously.[E6] In brief, PBMCs were isolated from heparinized blood of the patient and 10 age-matched control subjects (mean age, 22.7 years [SD, 4.62 years]) by using lymphocyte separation medium (MP Biomedicals, Santa Ana, Calif) and frozen in 10% dimethyl sulfoxide (Sigma, St Louis, Mo). Thawed cells were stained with eBioscience (San Diego, Calif) antibodies against CD3 (SK7), CD4 (RPA-T4), and IL-17 (eBio64DEC17). For cytokine staining, T cells were stimulated *ex vivo* for 5 hours in 50 ng/mL phorbol

12-myristate 13-acetate (Sigma) and 500 ng/mL ionomycin (Sigma) in the presence of GolgiStop (BD Biosciences) before staining. Before intracellular staining, cells were first surface stained as described, fixed, and permeabilized with Cytofix/Cytoperm (BD) for IL-17 stainings. Data were acquired on BD FACSCanto II and analyzed with FlowJo software (Tree Star, Ashland, Ore).

RESULTS

Salivary flow rate

The nonstimulated salivary flow rate in the index patient was less than 0.2 mL/5 minutes; the stimulated flow rate was 3.1 mL/5 minutes.

T385M is a gain-of-function mutation

On stimulation with IFN-α and IFN-γ, higher levels of STAT1 phosphorylation were observed by means of flow cytometry in the patient compared with those seen in a control subject (Fig 2, *B*). Next, we studied STAT1-binding activity to a GAS oligonucleotide probe by using EMSA. First, we studied the STAT1 phophorylation in skin-derived fibroblasts using Western blotting. We demonstrated an increased expression of total STAT1 in both the T385M patient (P1) and a second patient with CMC caused by a novel mutation in the DNA-binding domain (K388E; P2), although less pronounced than that in P2, compared with that seen in 2 healthy control subjects. Expression of phosphorylated STAT1 was increased in the nuclear extracts of both the T385M and K388E patients, although again less pronounced in the latter, after stimulation for 1 hour with IFN-γ. The phosphorylation of STAT1 in P1 and P2 was 7 and 2.7 times more intense than in C2 (Fig 2, *C*). On stimulation with IFN-γ, an increase in GAS-binding activity was detected in the T385M patient (P1; Fig 2, *C*), as well as in the K388E patient (P2). The intensity of STAT1-binding activity to a GAS probe was quantified to be 16.8 and 2.4 times upregulated in P1 and P2, respectively, compared with the intensity in C2, which was set to 1 in ImageJ software.

PBMCs of the patient do not induce IL-17

PBMCs of the patient do not induce IL-17 after stimulation with heat-inactivated *C albicans*, *S aureus*, or PHA. IL-17 in the supernatant was undetectable after stimulation with the above-mentioned stimuli (Fig E1, *A*). IFN-γ production after stimulation with PHA, heat-inactivated *C albicans*, and *S aureus* in the patient and a control subject are also shown (Fig E1, *B*).

Extended immunophenotyping at age 20 years

Using extended immunophenotyping, we showed that the patient has no detectable T_H17 cells.

REFERENCES

E1. Oftedal BE, Wolff AS, Bratland E, Kämpe O, Perheentupa J, Myhre AG, et al. Radioimmunoassays for autoantibodies against interferon omega: its use in the diagnosis of autoimmune polyendocrine syndrome type I. Clin Immunol 2008; 129:163-9.

E2. Denayer S, Helsen C, Thorrez L, Haelens A, Claessens F. The rules of DNA recognition by the androgen receptor. Mol Endocrinol 2010;24:898-913.

E3. Chapgier A, Boisson-Dupuis S, Jouanguy E, Vogt G, Feinberg J, Prochnicka-Chalufour A, et al. Novel STAT1 alleles in otherwise healthy patients with mycobacterial disease. PLoS Genet 2006;2:e131.

E4. Rasband WS. ImageJ. Bethesda: US National Institutes of Health. Available at: imagej.nih.gov/ij/.

E5. Borgers H, Moens L, Picard C, Jeurissen A, Raes M, Sauer K, et al. Laboratory diagnosis of specific antibody deficiency to pneumococcal capsular polysaccharide antigens by multiplexed bead assay. Clin Immunol 2010;134:198-205.

E6. Danso-Abeam D, Zhang J, Dooley J, Staats KA, Van Eyck L, Van Brussel T, et al. Olmsted syndrome: exploration of the immunological phenotype. Orphanet J Rare Dis 2013;8:79.

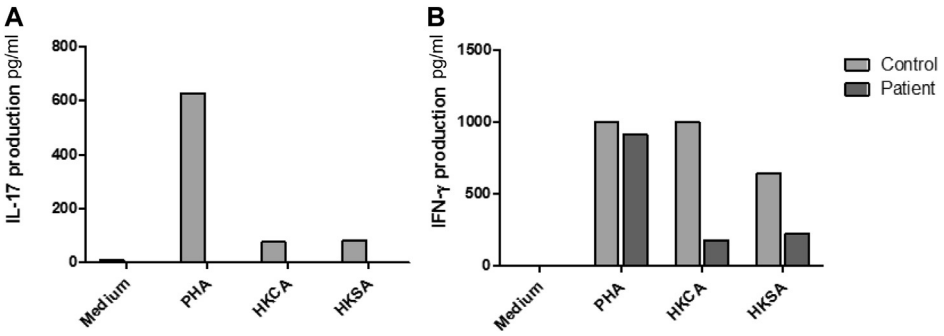

FIG E1. A, IL-17 production in PBMCs of the T385M patient and a healthy control subject after stimulation with PHA, heat-inactivated *C albicans*, or heat-inactivated *S aureus*. Results shown are derived from one representative experiment of 4 independent experiments. **B,** IFN-γ production in PBMCs of the T385M patient and a healthy control subject after stimulation with PHA, heat-inactivated *C albicans*, or heat-inactivated *S aureus*. Results shown are derived from one representative experiment of 4 independent experiments. *HKCA*, Heat-killed *C albicans*; *HKSA*, heat-killed *S aureus*.

TABLE E1. Clinical characteristics

Present age	**20 y**
Ethnicity	White
Initial presentation	At birth
CMC	Oral, esophageal, skin
Teeth	Retained primary dentition, severe caries and erosive tooth wear
Skin	Severe seborrheic dermatitis
Pulmonary infections	From birth
	Haemophilus influenzae, *Streptococcus pneumoniae*, *Pseudomonas aeruginosa*
	Aspergillus fumigatus
	Bronchiectasis at age 3 y, chronic obstructive pulmonary disease
Other infections	Molluscum contagiosum, *Pseudomonas* folliculitis, herpes zoster (2×)
Cardiovascular	−
Central nervous system	−
Endocrine	At birth: small for gestational age
	Growth retardation
	Delayed puberty
	Hypothyroidism (antibodies −) at age 18 y
Gastrointestinal	Oral aphthous ulcers, recurrent ulcerative gastritis, esophagitis
	Duodenal atrophic mucosa, villous blunting
	Diaphragmatic hernia
Bone	Osteopenia, multiple fractures
Other	Cystic fibrosis and primary ciliary dyskinesia were excluded.

TABLE E2. Specific anti-pneumococcal antibody concentrations (in milligrams per miter) in the patient 3 weeks after vaccination with unconjugated pneumococcal vaccine

	PS1	PS3	PS4	PS8	PS9N	PS12F	PS14	PS19F	PS23F	PS6B	PS7F	PS18C	PS19A	PS9V
Patient	0.28	0.37	2.33	0.20	1.31	0.38	6.37	2.71	5.44	4.11	1.35	2.52	0.91	2.81
Cutoff	0.53	0.64	0.49	1.02	0.63	0.46	0.57	0.74	0.24	0.80	1.45	0.34	0.96	0.69

The postvaccination serotype-specific fifth percentile *(Cutoff)* values obtained in 75 healthy subjects are provided as well. *PS*, Pneumococcal serotype.

TABLE E3. Immunologic characteristics

	Age 1 y	Age 3 y	Age 13 y	Age 20 y*
Lymphocyte subsets				
$CD19^+$ B cells			622/μL (82-476/μL)	
Naive $CD19^+CD27^-$ cells			94% of $CD19^+$ (60-80)	
IgM memory $CD27^+IgM^+$ cells			1.3% of $CD19^+$ (1-5)	
Switched memory $CD27^+IgM^-$ cells			1% of $CD19^+$ (>5)	
$CD3^+CD4^+$T cells			886/μL (455-1885 μL)	
$CD3^+CD8^+$ T cells			459/μL (219-1124/μL)	
Naive $CD4^+$ cells			75% of CD3 (30% to 65%)	
T_H17 cells				T_H17 cells 0% (0.03-0.67)
Lymphocyte proliferation				
PHA	Normal		Normal	
Concanavalin A	Normal		Normal	
Tetanus	Normal		Normal	
Candida	Normal		Normal	
Immunoglobulin levels (g/L)				
IgG		16.7 (4.8-11.3)	21.4 (5.8-12.7)	22.8 (7.51-15.60)
IgG_2		0.34 (0.72-3.40)	0.80 (1.06-6.10)	1.8 (1.5-6.4)
IgA		0.78 (0.35-1.9)	1 (0.81-2.32)	0.28 (0.82-4.53)
IgM		1.11 (0.34-1.34)	1.2 (0.30-1.59)	0.72 (0.43-3.04)

Normal values are shown in parentheses.
*During IVIG treatment.